Research on Engineering Structures & Materials
www.jresm.org
Research Group

Research Article

Thermomechanical properties of slag-based engineered geopolymer composite under a series of cooling and heating cycles

Ghassan H. Humur[1,a], Hussein Hamada[*2,b], Sarwar H Mohmmad[3,c], Abdulkadir Çevik[4,d], Farid Abed[5,e]

[1]*Department of Civil Engineering, University of Kirkuk, Kirkuk, Iraq*
[2]*Al-Qalam University College, Kirkuk 36001, Iraq*
[3]*Technical College of Engineering, Sulaimani Polytechnic University, Sulaymaniyah 46001, Iraq*
[4]*Department of Civil Engineering, Gaziantep University, Gaziantep, Türkiye*
[5]*Department of Civil Engineering, College of Engineering, American University of Sharjah, UAE*

Article Info

Article History:

Received 25 Aug 2024

Accepted 09 Jan 2025

Keywords:

Geopolymer composite;
Polyvinyl alcohol;
Polypropylene fiber;
Engineered cementitious composite;
Thermal cycling;
Microstructure

Abstract

Using Polyvinyl alcohol (PVA) fiber and micro silica sand has adverse effects on the economic and sustainable advantages of Engineered Geopolymer Composites (EGCs). This study suggests replacing PVA fiber with polypropylene fiber (PP) in producing sustainable reinforced slag-based-engineered geopolymer composites (SEGC) subjected to thermal cycling and repeated loads. PP and PVA fibers, with a 2% content as a volume fraction were selected to reinforce the EGCs. The study examined mass loss, microstructural characterization, static (monotonic) and cyclic loading measurements, tensile properties, and flexural properties. The results obtained indicate a substantial reduction in the strength of lightweight SEGC under thermal cycling. The density of LW-EGC and ECC composite ranged between 1758 for ECC and 1870 kg/m3 for PVA-EGC, while the statistic stress ranged between 37.35 for PVA-ECC and 63.78 for PVA-EGC. However, the flexural strength under static and cyclic loading of LW-ECC (LW-ECC) samples showed substantial improvement due to the increased reaction rate of fly ash particles under high temperatures. Microstructure analysis revealed that SEGC samples suffered more severe damage than ECC specimens when subjected to various cooling and heating cycles. These micro-cracks contributed to defects in the residual mechanical behavior of lightweight SEGC specimens.

1. Introduction

During In recent times, there has been an increase in the popularity of ductile fiber-reinforced geopolymer composites (DFRGC) in various construction applications [1, 2]. However, these composites are susceptible to exposure to different environmental factors during their curing process and service life, including heat and cooling cycles, fire incidents, freeze and thaw cycles, weather deterioration, and chemical attacks [3, 4]. These factors can pose significant risks to the performance and longevity of these materials in construction projects. Building components are subject to temperature variations throughout their lifespan, ranging from sub-zero degrees Celsius to approximately 80°C, depending on the geographical location. As a result, assessing the durability

*Corresponding author: enghu76@gmail.com
[a]orcid.org/0000-0002-4915-2887; [b]orcid.org/0000-0001-9911-8639; [c]orcid.org/0000-0002-7249-7760; [d]orcid.org/0000-0001-6700-0126; [d]orcid.org/0000-0002-9202-694X
DOI: http://dx.doi.org/10.17515/resm2025-412me0825rs

and service life of construction elements must take into account the effects of thermal cycling, which is a crucial aspect of evaluating serviceability in the construction industry.

Ping et al. [5, 6] conducted a study to investigate the performance of fly ash in geopolymer concrete (FAGPC) under the influence of cooling and heating cycles. The researchers studied the influence of adding Iron ore tailing (IOT) and Silica fume (SF) in different ratios of 0%, 10%, 20%, and 30% by weight. The FAGPC specimens mixed with varying IOT and SF content were subjected to heating and cooling sequences for 7, 28, and 56 days at temperatures of 200, 400, and 800 °C. The study focused on recording the residual mechanical properties, weight loss, and microstructural characteristics of the specimens. The addition of SF and IOT led to the refinement of pores in the geopolymer and the optimization of microstructural cracks under thermal cycling. As a result, there was a reduction in porosity and micro-cracks, leading to an increased density of the microstructure and enhanced thermal resistance of the FAGPC specimens [7]. However, it was observed that the FAGPC specimens experienced an increase in mass and a loss of compressive strength, especially after undergoing 56 thermal cycles. Another study by Lin et al. [8], observed that thermal cycles hurt gas permeability. This effect was attributed to the enlargement of pores within the aggregates and cementitious materials. An et al. [9] examined the microstructural and mechanical behavior of high-performance concrete (HPC) under different thermal cycling conditions. The evaluation of HPC involved analyzing parameters such as compressive strength, elastic modulus, capillary water absorption, and splitting tensile strength. The researchers observed that as the number of heating and cooling cycles increased, there was a decrease in the compressive strength, splitting tensile strength, and elastic modulus of high-performance concrete (HPC). The uniaxial tensile test of HPC under varying strength grades was particularly sensitive to thermal treatment. With an increase in the number of thermal cycles, macroscopic cracks were observed in HPC, leading to weakened performance. This crack propagation was attributed to the existence of micro-cracks in the cement matrix and interfacial transition zone.

Geopolymers are a new type of inorganic material without cement, alkali-activated structure that has gained substantial attention in sustainable construction [10]. İt was produced from different aluminosilicate materials like slag and fly ash with alkali solutions like sodium or potassium hydroxide and silicate [11, 12]. Geopolymer and other cementitious materials have gained popularity due to their sustainability. Alkali-activated materials have been used as a replacement for Ordinary Portland Cement (OPC) and consist of aluminosilicate materials like slag and fly ash (FA) at normal or elevated temperatures [13]. Geopolymer composites have been found to reduce carbon footprint by about 80% and decrease the energy required by 60% compared to clinker-based cement production [14]. Engineered Geopolymer Composites (EGCs), a novel type of ductile fiber-reinforced geopolymer composite, contain a small ratio of short fibers (2% by volume) [15]. These materials offer significant advantages, such as being eco-friendly, reducing greenhouse gas emissions, and exhibiting high strain in uniaxial tensile tests. The use of landfill materials like fly ash, rice husk ash, and slag contributes to greener production with a lower carbon footprint and reduced environmental hazards [16]. Strain-hardening geopolymer composites display a high deformation capacity of about 74.3 mm and a relatively high flexural strength of approximately 12.7 MPa, demonstrating strong deformation performance [17]. Additionally, they exhibit high tensile ductility (up to 4.69%) and compressive strength (up to 64.11 MPa) [18].

Alrefaei and Dai [15] conducted an evaluation of the influence of combined fibers on the microstructural and tensile strength properties of one-part EGC treated at controlled temperatures. They studied the impact of hybrid combinations of steel fiber (SF) and polyethylene fiber (PE), with different precursor material ratios (100% slag and 50% FA-50% slag), along with the addition of micro-silica sand. The results revealed that the addition of steel fibers in the EGC composites led to an increase in dry density, slump, compressive strength, and fracture properties. However, it also resulted in a considerable decrease in the tensile strain and led to the formation of cracks in both hybrid mixes of EGC. In a separate study, Ling et al. [18] investigated the effect of the strong bond and slag content on the properties of EGC containing FA. The outcomes showed the presence of numerous small cracks in all EGC specimens. The inclusion of slag in EGC composites increased the spacing between cracks while reducing their number. During tensile loading and flexural strength tests, all EGC samples, regardless of slag content, exhibited fine cracks.

However, the presence of slag reduced the number of cracks and increased the spacing between them.

Another study by G. Humur and A. Çevik [19] reported on the impact of high temperature on the deflection and strain-hardening behavior of EGC. The load-deflection responses showed that both ECC and EGC specimens maintained their deflection-hardening behavior at a thermal treatment of 200°C. Additionally, slag/fly ash-based EGC and fly ash-based EGC composites demonstrated higher flexural strength and deflection properties at 100°C and 200°C compared to control samples heated under normal conditions. However, the flexural strength and deformation properties of all EGC and ECC specimens degraded with increasing heat treatment up to 800°C. G. Humur and A. Çevik also investigated the effects of nano-silica, PP, and PVA fibers in slag/fly ash-based lightweight EGC (S-FA-EGC) [7]. The incorporation of polypropylene fibers in lightweight S-FA-EGC specimens enhanced tensile ductility and reduced tensile stress at ambient temperature. Moreover, the reinforcement of lightweight S-FA-EGC specimens with polyvinyl alcohol fibers eliminated fragmentation and explosive spalling, significantly enhancing the fire resistance of ECC and EGC under high temperatures. This is because the melted fibers create additional routes for vapor pressure to escape without damaging the EGC and ECC matrices [7].

To date, limited studies have investigated the influence of slag-based EGC under elevated temperatures. Most studies have focused on normal EGC, while the behavior of reinforced slag-based LW-EGC (SEGC) under cyclic heating-cooling programs has not been widely explored. Therefore, it is essential to study the changes in microstructural evolution and engineering properties of SEGC. Additionally, the influence of thermal cycles on the behavior of conventional ECC has not been extensively studied in the literature. This study aims to systematically examine the behavior of SEGC reinforced with polypropylene and polyvinyl alcohol fibers that are exposed to cooling-heating cycles (room temperature and 10, 20, and 30 cycles.) The study examines the influence of combined fibers on mass loss, density, static (monotonic) and cyclic loading responses, failure mode, strain hardening behavior, deflection hardening behavior, and microstructural characterization of lightweight SEGC and ECC composites. The outcomes acquired from this study will provide a fundamental database of the durability properties and mechanical behavior of SEGC exposed to heating-cooling cycles.

2. Experimental Program

2.1 Materials and Mix Preparations

In this research, ground granulated blast furnace slag (GGBFS) was chosen to produce lightweight SEGC mixes, while Ordinary Portland Cement (OPC) and low calcium fly ash (FA) were used to create LW-ECC as control samples. Table 1 provides the chemical composition and physical properties of GGBFS, OPC, and FA analyzed through X-ray Fluorescence (XRF). Expanded glass granule aggregate (EGGA) from HAbbe, a company located in the Kocaeli region of Turkey, was adopted as the fine aggregate in all concrete mixes. EGG is characterized by its creamy or white color, with a breaking resistance, bulk density, and granular size of 3.1 N/mm2, 450 kg/m^3, and 0.1-0.25 mm, respectively. NaOH and water glass were selected as alkaline activators for this study.

Table 1. Properties of OPC, GGBFS, and FA%

Chemical composition	GGBFS %	FA %	OPC %
SiO_2	36.4	62.53	19.69
CaO	34.12	1.57	62.12
Al_2O_3	10.39	21.14	5.16
MgO	10.3	1.76	1.17
Fe_2O_3	0.69	7.85	2.88
Na_2O	0.35	2.45	0.17
K_2O	0.97	0.73	0.88
SO_3	0.49	0.10	2.63
Loss on ignition %	1.64	2.07	2.99
Blaine fineness (m^2/kg)	418	227	394

Specify gravity	2.79	2.04	3.15

One day before casting, a 12 M NaOH solution was prepared, and a water glass with a molar ratio (Ms) of 3.10 was also prepared before the casting process. The Na2SiO3/NaOH ratio was set at 2.5 to fix the alkaline activator solutions. Table 2 presents the XRF analysis of the EGG materials. Polypropylene (PP) fibers with a length and diameter of 12 mm and 40 μm, respectively, were employed. Additionally, polyvinyl alcohol (PVA) fibers with a diameter of 39 μm, a volume fraction of 2%, and a length of 12 mm were used in this study. Table 3 provides the properties of PP and PVA fibers. A polycarboxylate-based high-range water-reducing admixture (PHRWRA) was used to improve the workability of the concrete mixes.

Table 2. Chemical composition of EGGA

Constituent	%
SiO_2	72.95
CaO	4.35
MgO	0.89
Al_2O_3	0.41
Fe_2O_3	0.09
Mn_2O_3	0
TiO_2	0.03
K_2O	0.2
Na_2O	18.74
Loss on Ignition (LOI)	2.33

Table 3. Characteristics of PVA and PP fibers

Type of fiber	Diameter (μm)	Length (mm)	Aspect ratio	Specific density (g/cm^3)	Elastic modulus (GPa)	Tensile strength (MPa)
PP	40	12	300	0.91	5	450
PVA	39	12	300	1.30	42.8	1620

Table 4 presents the mix proportions for LW-ECC and EGC. The Na_2SiO_3/NaOH ratio was fixed at 2.5 for all LW-EGC mixes, and the proportion of alkali activator/binder was maintained at 0.45. The proportion of EGG to binder was also set at 0.2 to ensure that the overall combinations have a density lower than that of the control mass. In total, six mixes were included in the testing program. Mix proportions Mix1, Mix2, and Mix3 were prepared to investigate the effect of microfibers (PVA and PP) on the properties of slag-based LW-EGC when exposed to thermal cycling. These mixes included different fiber contents while keeping a total volume of 2%. Additionally, two mixes without PVA and PP fibers were prepared to examine the influence of fiber type on the physical, thermal, and mechanical properties of SEGC and ECC composites.

Table 4. Characteristics of LW- ECC and EGCs mixtures (units)

Mixtures	GGBFS	FA	OPC	NaOH	Na_2SiO_3	Liquid/ binder	Sand/ binder	PP	PVA	Extra water	HRWR
PP-EGC	1.0			0.128	0.321	0.45	0.2	0.02		0.02	0.025
PVA-PP-EGC	1.0			0.128	0.321	0.45	0.2	0.01	0.01	0.02	0.035
PVA-EGC	1.0			0.128	0.321	0.45	0.2		0.02	0.02	0.046
PVA-ECC		0.5	0.5			0.29	0.2		0.02	0.02	0.02
EGC	1.0			0.128	0.321	0.45	0.2			0.018	0.025
ECC		0.5	0.5			0.29	0.2			0.018	0.02

2.2 Mixing and Curing

To prepare the NaOH solution with the desired molarity of 12M, accurately weighed sodium hydroxide beads were dissolved in drinking water. As the ingredients were mixed, an exothermic reaction occurred, leading to an increase in temperature. The solution was allowed to reach its equilibrium state at room temperature before use. This step is crucial to ensure the proper preparation of the NaOH solution. Next, the required materials were dried for about six minutes. Afterward, additional water with the alkaline activator solution was added to the LW-SEGC mix. Wet mixing was carried out for 3 minutes to ensure proper distribution. The polycarboxylate-based high-range water-reducing admixture (PHRWRA) was gradually added to obtain a workable mix. PVA fibers were incorporated and mixed for another six minutes until a homogeneous mix was achieved. The entire mixing process took approximately 15-20 minutes for each mix proportion.

The lightweight SEGC and ECC mixes were then cast and properly compacted using a vibrating table for 1 minute. In this study, an oven was chosen for the curing process, as previous research has shown that oven curing enhances the tensile ductility and mechanical properties of EGC [20, 21]. Fresh SEGC samples were wrapped to prevent moisture loss and placed in the oven at 70°C for 24 hours. Then, all SEGC samples were removed from the oven and kept at ambient room temperature. As for the LW-ECC samples, they were demolded after the 24-hour resting period and submerged in a water bath for 28 days.

2.3 Test Program

2.3.1 Compressive Strength

The compressive strength test of LW-ECC and EGC specimens was conducted using ASTM C109 [20] standards. The concrete cubes had dimensions of 70 × 70 × 70 mm^3, and at least three specimens were tested to obtain an average result.

2.3.2 Direct Tensile Strength

For the tensile strength test, coupon specimens with dimensions of 330 mm x 60 mm x 13 mm were utilized to assess the tensile properties of the lightweight composites. The test was conducted at a loading rate of 0.2 mm/min to control the deformation, following the guidelines of the Japanese code [22].

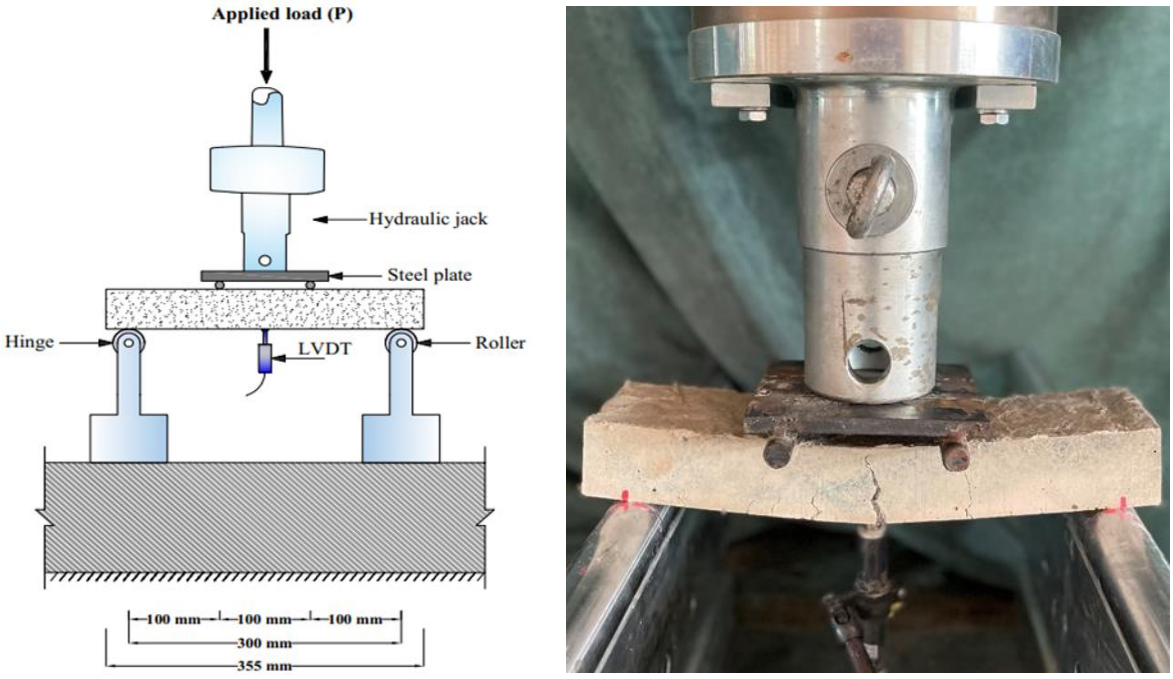

(a) (b)

Fig. 1. Test set of four-point flexural test (a) Test set up and (b) SEGC specimen

2.3.3 Flexural Strength

To assess the flexural strength, the lightweight composites were subjected to a four-point bending test using prism specimens with dimensions of 50 mm x 76 mm x 355 mm at a loading rate of 0.2 mm/min, as specified in previous studies [23]. Fig. 1 illustrates the flexural testing machine used, with a capacity of 500 kN.

2.3.4 Scanning Electronic Microscopy

After mechanical testing, scanning electron microscopy was used to investigate the reason for changes in the strength of SEGC and ECC microstructures after exposure to various thermal cycles. SEM technique (ZEISS Gemini SEM 300) was adapted to assess the changes in the microstructure of all studied samples under thermal cycles, as shown in Fig.2.

Fig. 2. SEM device

2.3.5 Exposure to Thermal Cycling

In order to examine the behavior of the specimens under thermal cycling, all the tested samples were subjected to high temperatures up to 200°C at 28 days of age. Subsequently, the specimens were slowly cooled back to room temperature. Each heating and cooling cycle was considered as one step of thermal curing. The mechanical properties of the SEGC and ECC composites were evaluated at intervals of 10 cycles up to a maximum of 30 cycles. At the age of 28 days, all the lightweight SEGC specimens were subjected to a temperature of 200 °C in a computer-controlled, electrically heated furnace at a heating rate of 10°C/minute till the target temperature was attained and the temperature was maintained constant for 2 hr (heating time) After that, the samples were allowed to cool naturally to ambient temperature (cooling time). This heating-cooling cycle is hereafter referred to as one thermal cycle.

3. Results and Discussions

3.1 Microstructural Analysis

To gain detailed insights into the influence of cooling and heating cycles on the microstructural behavior of SEGC and ECC specimens, Scanning Electron Microscopy (SEM) analysis was conducted on cores extracted from 70 mm specimens. These specimens were cured at room temperature, subjected to 10 thermal cycles, and subjected to 30 thermal cycles before compressive strength testing. Figure 3 presents the SEM images of LW-ECC and SEGC composites at different thermal cycles. The integration of slag in the EGC mix appears to improve the density of the matrix and decrease the void ratio of the EGC mix (Fig. 3a, b, and c). The microstructure of LW-ECC specimens also contains several unreacted fly ash (FA) particles in spherical forms. When these LW-ECC specimens are exposed to various cooling and heating cycles at a temperature of 200°C, it significantly affects the microstructural properties. On the other hand, the ECC mix exhibits a

homogeneous and well-compacted microstructure. Furthermore, the materials undergo accelerated chemical reactions and leaching due to thermal cycling.

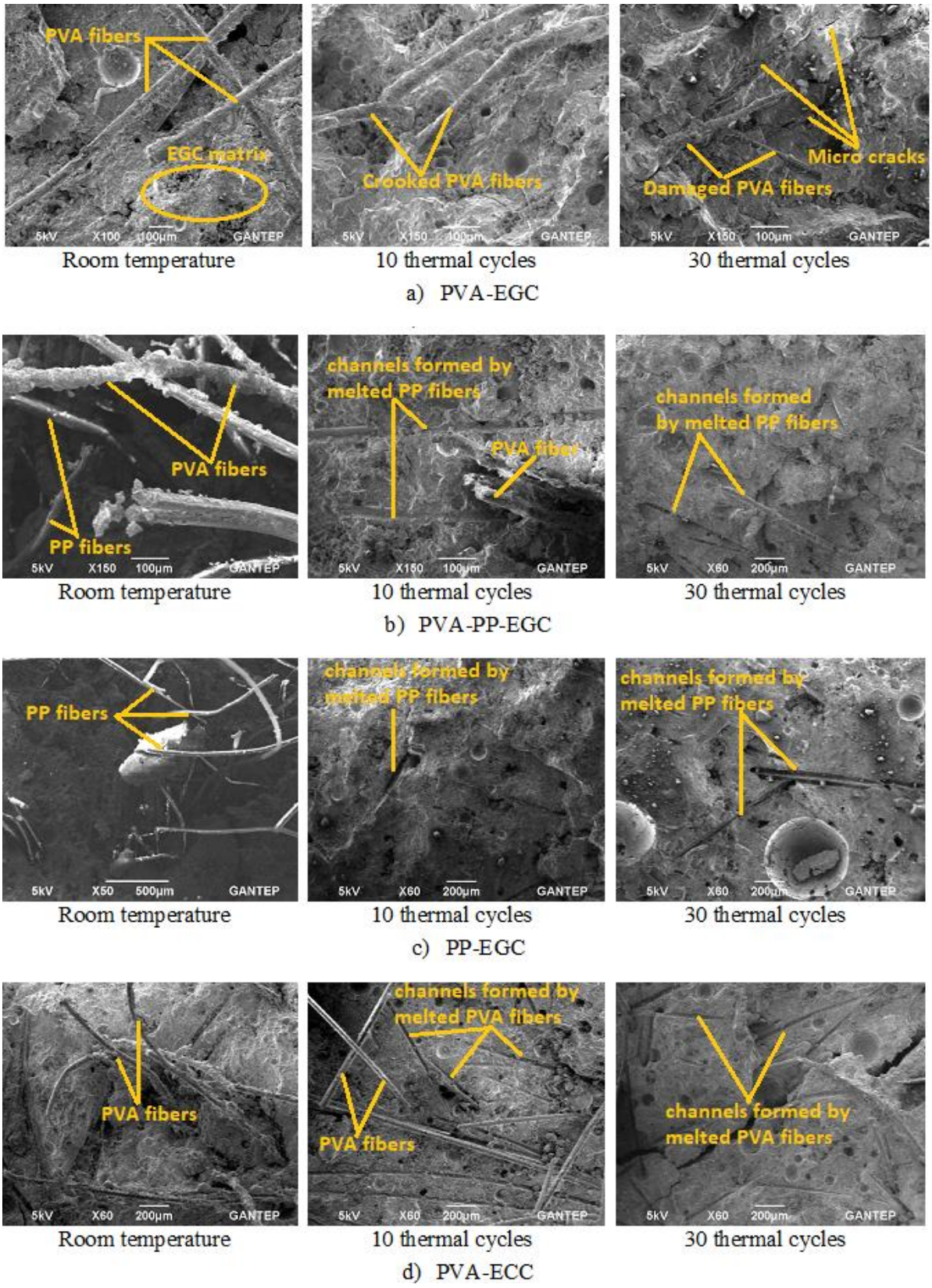

Fig. 3. SEM images of the green LW (ECC and EGC) composites both before and after being subjected to heating-cooling cycles

The spreading of fibers in the PVA-EGC specimens appears to be more homogeneous compared to the PP-EGC and PVA-PP-EGC specimens. As a result, the PVA fiber-reinforced specimens exhibit

higher mechanical properties than the specimens reinforced with PP fibers, as reported by previous studies [24, 25]. The thermal cycling treatment somewhat affected the PVA-EGC and PVA-ECC specimens. The PVA fibers did not melt when exposed to the thermal cycles between 10 and 30 cycles, particularly at 200 °C. On the other hand, the PP fibers in the PP-EGC specimens completely melted and disappeared after 10-30 thermal cycles, resulting in a noticeable significant number of capillary pores and micro-cracks in the microstructure. This is attributed to the low softening point of PP fibers, which induces minor cracks in the EGC mix and adversely affects the residual strength of LW-EGC specimens (Fig. 3b and c).

In the case of the microstructure of PVA-PP-EGC, no significant modification was observed after heat treatment until approximately 10 thermal cycles. However, after 30 cycles, an increase in crack spacing was observed in the hybrid composite. Channels may form, and cracks may develop as a result of PP fiber melting. This suggests that the microstructure of the hybrid composite is influenced at this stage, and additional cracks were observed on the surface of the specimens (Fig. 3b). The porosity considerably increased, and interconnected open pores were observed after 30 thermal cycles. The increased porosity and pore connectivity in the microstructure of the specimens are attributed to the softened PP fibers, resulting in a notable degradation in the strength of LW-EGC specimens. Compared to PVA-EGC specimens, PP-EGC specimens exhibited higher porosity and additional micro-cracks, mainly due to the melting of PP fibers within the SEGC matrix. This results in an increase in porosity and voids within the EGC mix, leading to structural flaws and a considerable loss in strength due to thermal treatment [26]. The micromorphology of PVA fibers in PVA-ECC and PVA-EGC samples deteriorated when exposed to higher heating and cooling cycles, and their microstructure was somewhat affected, with additional surface irregularities observed on the specimens (Fig. 3a and d). However, PVA-EGC specimens exhibited greater damage compared to PVA-ECC specimens after 30 thermal cycles. This is attributed to the higher number of voids and greater porosity in the microstructure of ECC compared to SEGC, which makes the internal microstructure of ECC less susceptible to the impact of thermal treatment. After being subjected to various thermal cycles, the higher the cooling and heating cycles, the course the pore structure and the higher the total intruded porosity of SEGC and ECC mixtures. Sahmaran and Li (2010) stated that the average pore diameter of ECC specimens dramatically enlarges to 2–10 times its original size after ECC has been exposed to 400 and 800°C. microstructural analyses revealed that physical change (increase in total intruded porosity, the average pore diameter, and surface cracking was greatly changed after the exposure of ECC composites to different temperatures.

3.2 Characteristics of Compressive Strength Under Static and Cyclic Loading

Table 5 presents the properties of static and cyclic loading of SEGC and ECC specimens at room temperature. The average test results, based on at least three specimens, are provided. The findings indicate that thermal cycling has a positive influence on the compressive strength of ECC mortar samples (without fiber), while SEGC samples experienced a significant strength loss with an increase in thermal cycles. The retained strength of ECC specimens can be attributed to the sintering process of non-reacted fly ash particles, which contributes to the strength improvement of ECC specimens [27]. The influence of fiber type on static and repeated loads is illustrated in Figure 4. The compressive strength of SEGC specimens gradually decreases with an increase in polypropylene fiber content. For example, the behavior of static and cyclic loading for both PP-EGC and PVA-PP-EGC specimens decreases by approximately 10% 40.1%, 13.1%, and 41.5%, respectively. When comparing the static and cyclic loading of PP-EGC and PVA-EGC specimens, it is evident that PVA fibers, with their higher modulus of elasticity compared to PP fibers, exhibit outstanding elongation and bridging connections at the fiber breakage points. These PVA fibers can absorb the energy generated by matrix cracking, preventing crack propagation and contributing to high mechanical properties [27, 28].

The residual strengths of PVA fiber-reinforced specimens were higher compared to specimens reinforced by PP fibers after being subjected to various thermal cycling conditions. The partially improved mechanical features of PVA-EGC specimens were observed after being removed from the oven and cooled to room temperature. Conversely, PP fibers melted totally and reduced its

strength. Additionally, the residual compressive strength of LW-ECC specimens significantly improved with an increase in the number of heating and cooling cycles. The static and cyclic loading of PVA-ECC specimens increased from 37.35 MPa to 51.02 MPa and from 36.86 MPa to 48.29 MPa, respectively, as the number of thermal cycles increased from 0 to 10. The improvement in compressive strength can be attributed to the large amount of fly ash in the LW-ECC mix, which undergoes a pozzolanic reaction even after 28 days. The reaction of fly ash is enhanced through thermal curing, resulting in improved compressive strength [21]. The residual strengths of LW-ECC specimens subjected to 20 and 30 thermal cycles remain higher than that of unheated specimens, owing to the existence of a large number of voids and a more permeable microstructure in the ECC mix. This mitigates the influence of thermal curing on the microstructure of the ECC matrix and serves as a protective coating for preserving the integrity of the PVA fibers against the effects of thermal curing.

Table 5. Density, cyclic, and static compressive strength of LW-EGC and ECC composite

mix code	Density (Kg/m^3)	Static stress MPa	Cyclic stress MPa
PVA-EGC	1870	63.78	62.24
PVA-PP-EGC	1848	57.96	55.02
PP-EGC	1839	45.51	43.97
PVA-ECC	1790	37.35	36.86
EGC	1799	51.02	48.64
ECC	1758	41.25	37.85

PVA-EGC exhibits the highest compressive strength among the EGC composites, often reaching 60 MPa for high-strength concrete [29]. However, in the case of slag-based LW-EGC mixes, the cement content is reduced, distinguishing it from typical high-strength concrete. As a result, it has a significantly reduced environmental footprint compared to high-strength concretes (HSC) [29]. The strengths of LW-PVA-EGC specimens for both static and cyclic loading are 70.8% and 68.9% higher, respectively than that of the corresponding lightweight PVA-ECC specimens.

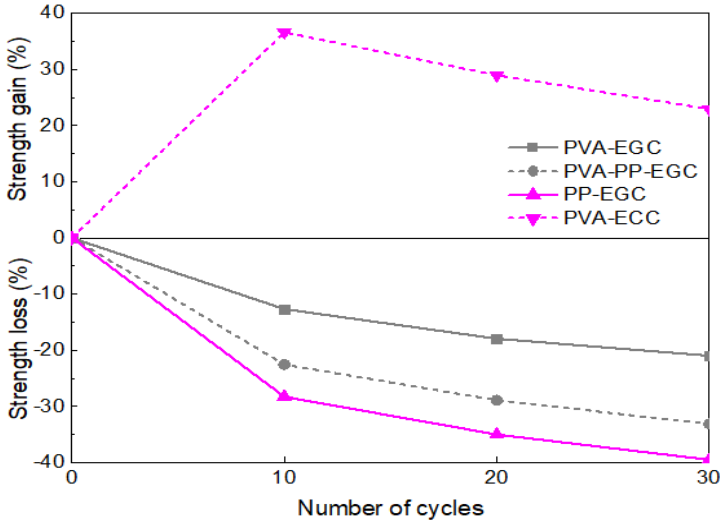

Fig. 4. Compressive strengths improvement and loss of green LW-ECC and LW-EGC specimens subjected to different thermal cycles

The significant effect of slag on the compressive strength of LW-EGC can be attributed to its improved cementing properties compared to FA. The high amount of CaO has a significant effect on the early strength development of concrete [30]. Additionally, the high CaO content can contribute to the formation of C-S-H/C-A-S-H gels, which can alter the microstructural elements of the EGC mix and further improve its strength [31]. The development of C-A-S-H gels also reduces the porosity and improves the microstructure of the EGC mix [32]. These findings are consistent with the SEM observations of LW-EGC composites mentioned earlier (section 3.1).

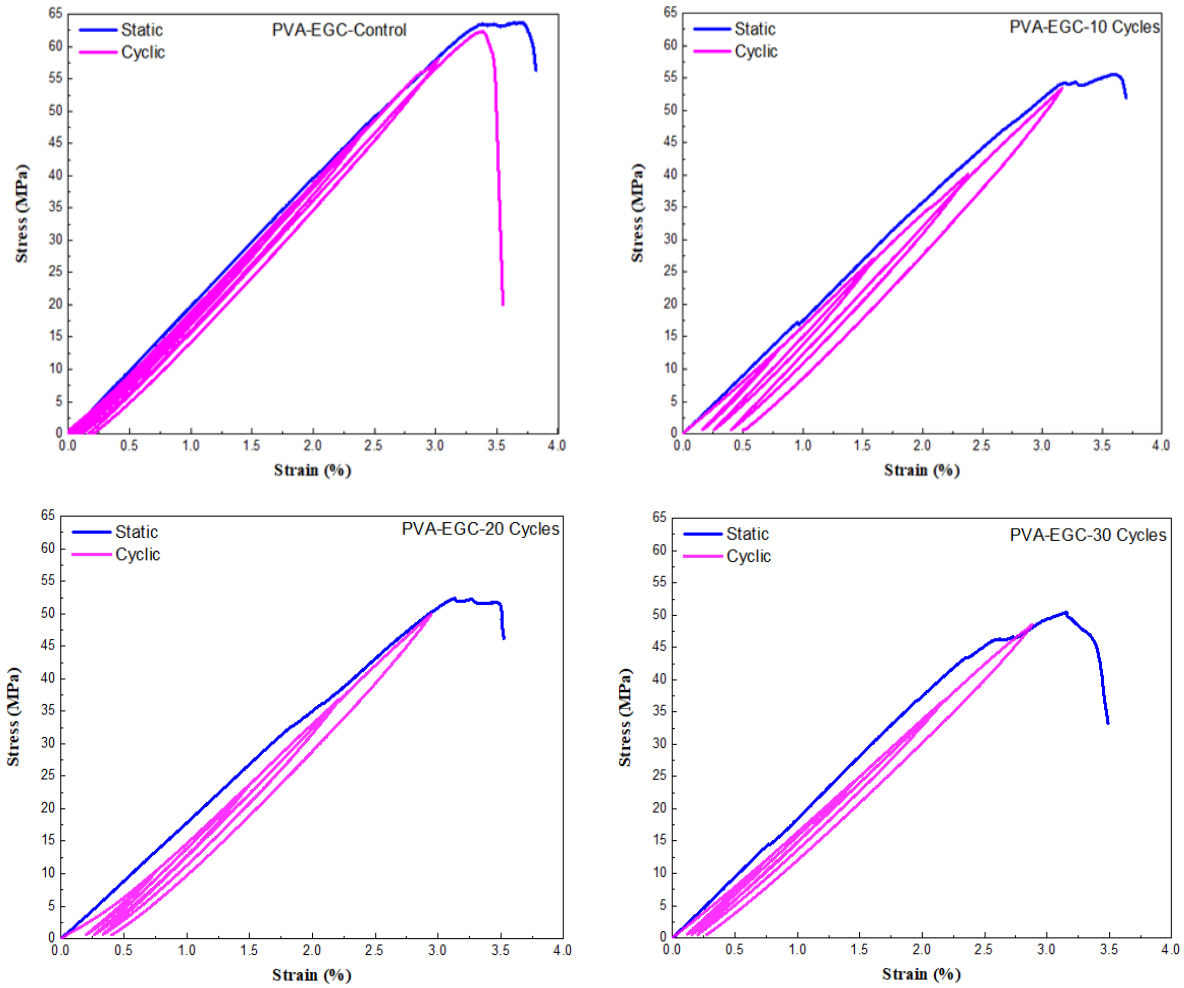

Fig. 5. Static and cyclic stress strain responses for PVA-EGC specimens at different thermal cycles

Figures 5-8 depict the influence of thermal cycling on the stress-strain behavior of the green LW-EGC and ECC specimens under static and cyclic loading. The behavior of both LW-ECC and EGC specimens exhibited nearly linear pre-peak behavior up to the maximum loads, even for specimens subjected to thermal cycles. Minor deviations were observed in the post-peak region of the static and cyclic curves for both lightweight specimens, as the elastic modulus decreased with increasing loading/unloading cycles. Similar properties have been reported in previous studies [33, 34]. Upon investigating the LW-EGC specimens under cooling and heating cycles, it was observed that both static and cyclic loadings decreased as the number of thermal cycles increased. The strength of PVA-PP-EGC, PP-EGC, and PVA-EGC specimens decreased by 28%, 23%, and 13%, respectively, after 10 thermal cycles. Further deterioration in the compressive strengths of LW-EGC specimens was observed as the heating and cooling cycles increased from 10 to 30. This reduction is due to the dense mix of the slag-based EGC, which promotes the accumulation of vapor pressure, leading to internal cracking. The different particle sizes, irregular flake-shaped particles, and high density of slag contribute to the denser microstructure of the slag-based EGC mix, resulting in reducing the pore size and thickness of the interfacial transition zone (ITZ) between PVA fibers and the EGC matrix. Additionally, the melting point and thermal cycling of polypropylene fibers significantly degrade the quality of the materials. Polypropylene fibers melt totally at a temperature of about 160 °C, rendering them unable to mitigate the detrimental effect of micro-cracks. The existence of voids in melted fiber in the EGC mix effectively decreases the compressive strength [35].

Figure 9 illustrates the failure modes of the green LW-ECC and EGC specimens after subjecting to various heating and cooling cycles. Irrespective of the compound type, the specimens exhibited a higher level of reliability before undergoing thermal curing owing to the inclusion of PP and PVA fibers in their mix proportions. The specimens reinforced by PVA fibers showed a more aggressive

failure compared to the specimens reinforced with PP fibers, primarily due to the high bond availability provided by the PVA fibers. This resulted in cracks propagating throughout the mid-lengths of the specimens. During thermal treatment, the failure pattern of the PVA fiber-reinforced specimens remained consistent with increasing thermal cycles, maintaining the integrity of the specimens.

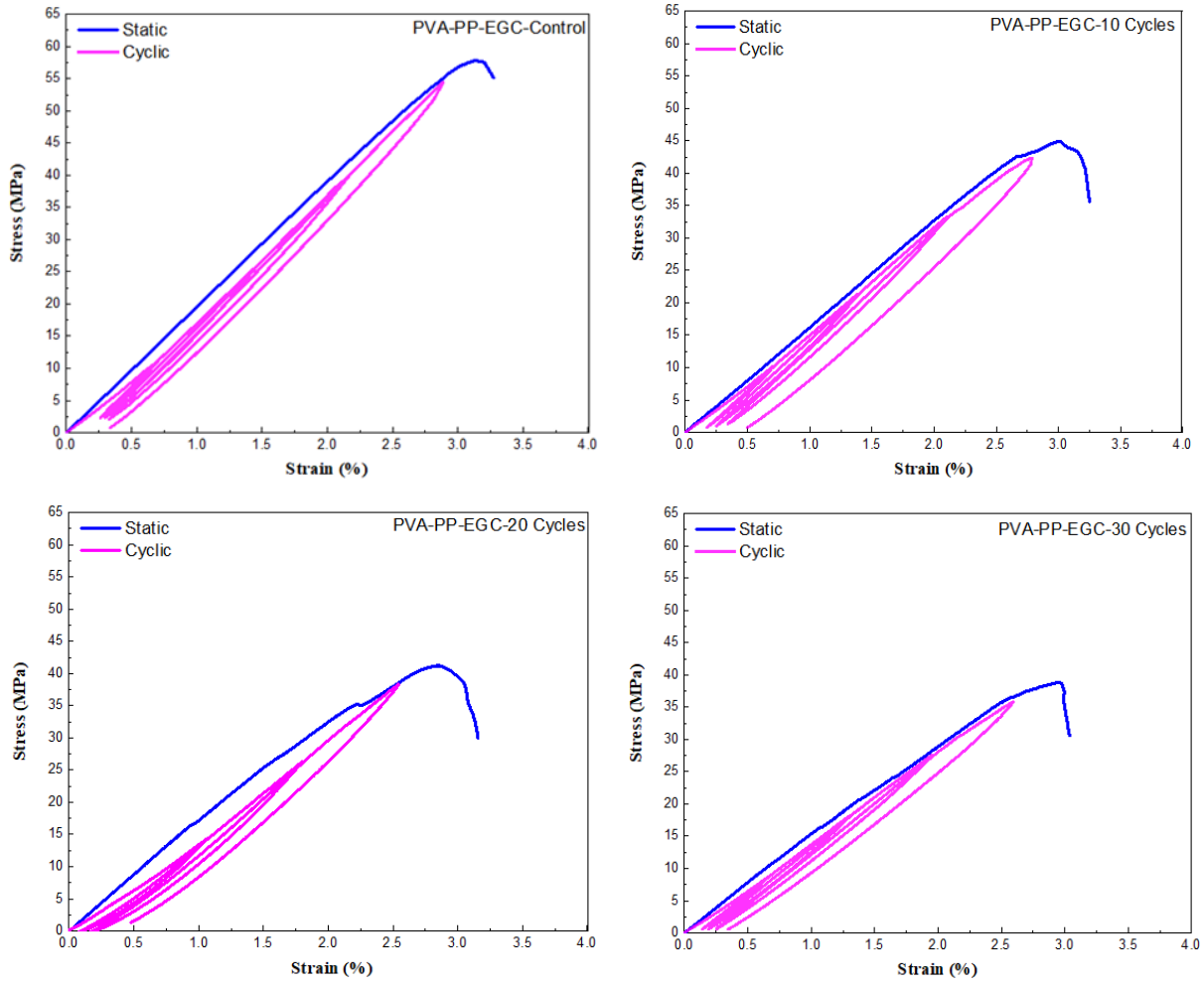

Fig. 6. Static and cyclic stress strain responses for PVA-PP-EGC specimens at different thermal cycles

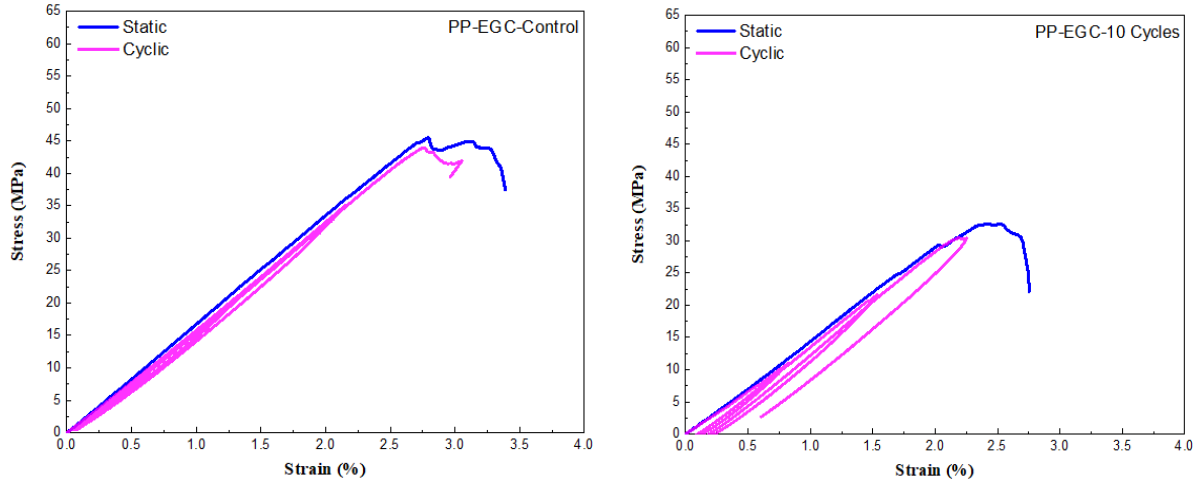

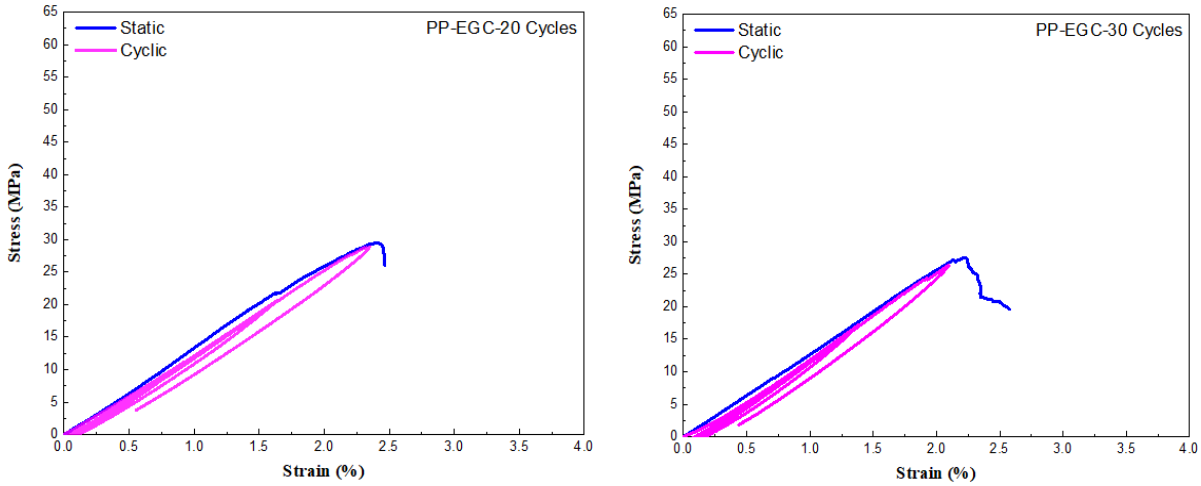

Fig. 7. Static and cyclic stress-strain responses for PP-EGC specimens at different thermal cycles

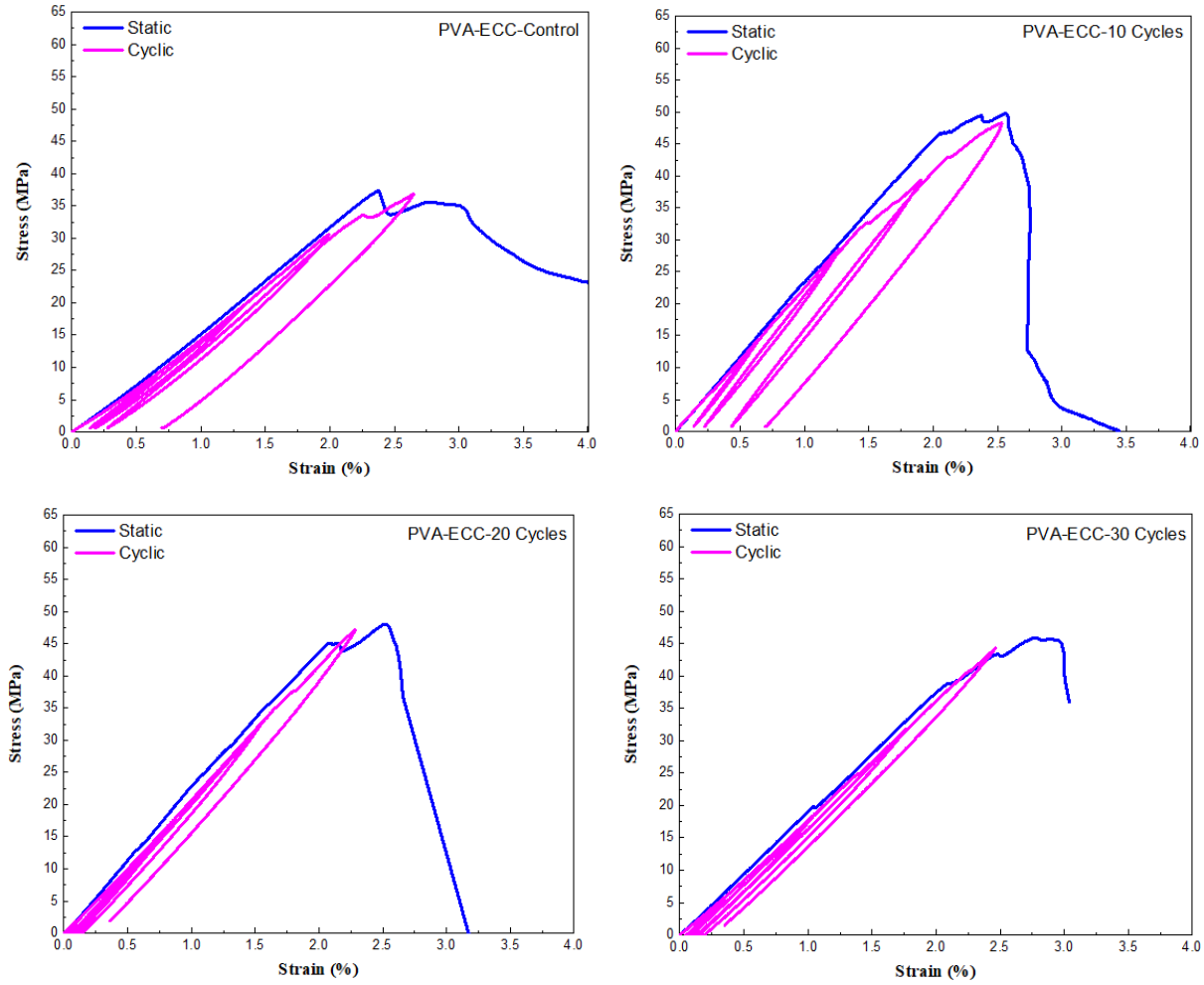

Fig. 8. Static and cyclic stress-strain responses for PVA-ECC specimens at different thermal cycles

However, instead of major cracks, finer cracks were visibly detected during the compression test due to the partial breakage of PVA fibers under thermal curing, resulting in a weakened bond between the EGC matrix and the PVA fibers. On the other hand, the specimens reinforced with PP fibers experienced severe fragmentation and exhibited brittle properties when exposed to high temperatures. This is due to the complete melting of PP fiber at a temperature of 160 °C. This change in failure mode from ductile to brittle properties is in agreement with the literature that applied PP fibers in their studies [33, 36].

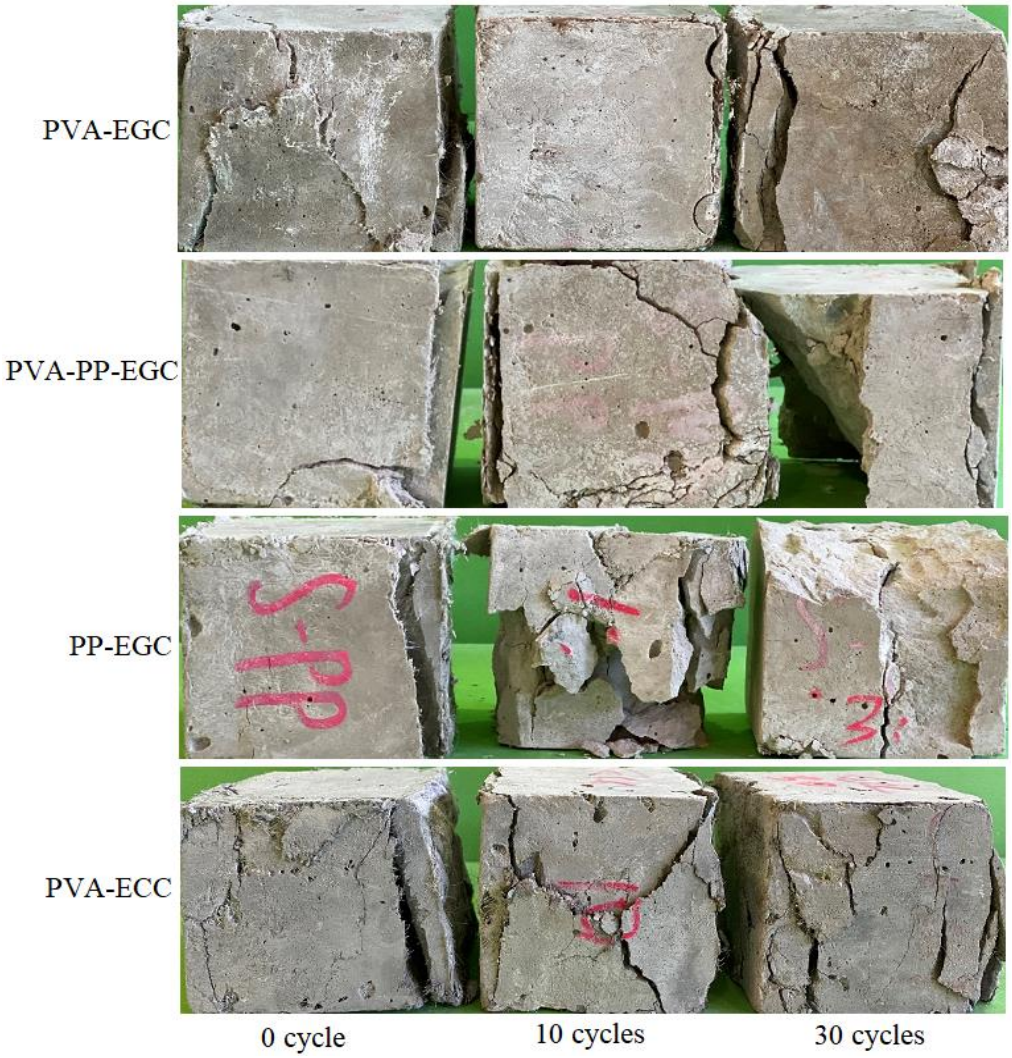

Fig. 9. The failure shape of green LW-ECC and LW-EGC specimens at compression test under different thermal cycles

3.3 Tensile test

Direct tensile tests were conducted to examine the stress-strain and tensile strength responses of the LW-ECC and LW-EGC composites under heating and cooling cycles, as presented in Fig. 10. Overall, all specimens showed strain hardening behavior, with crack propagation and narrow crack widths. The ultimate tensile strength of both ECC and EGC composites before thermal curing was significantly higher than the first crack strength. It was observed that at room temperature, the tensile strength of PP-EGC, PVA-PP-EGC, and PVA-EGC composites was 2.17 MPa, 4.28 MPa, and 4.97 MPa, respectively, with strain capacities of 2.09%, 1.43%, and 1.90%.

The results showed that PVA fiber-reinforced specimens exhibited higher tensile stress, but lower tensile ductility compared to specimens reinforced with PP fibers. The tensile stress of PVA-EGC specimens was 229% higher than that of PP-EGC specimens, while the ductility of PP-EGC specimens was 10% higher than that of PVA-EGC specimens. The use of inexpensive polypropylene fibers in LW-EGC composites demonstrated improved strain behavior. However, the tensile strength of PVA-EGC samples was 10 times higher than that of PVA-ECC specimens, while the strain capacity of PVA-EGC specimens was 22% lower than that of PVA-ECC specimens. This increase in tensile ductility of LW-ECC composites was attributed to the incorporation of FA binder, which reduced the bond between the PVA fibers and ECC matrix, resulting in higher ductility and lower fiber bridging strength.

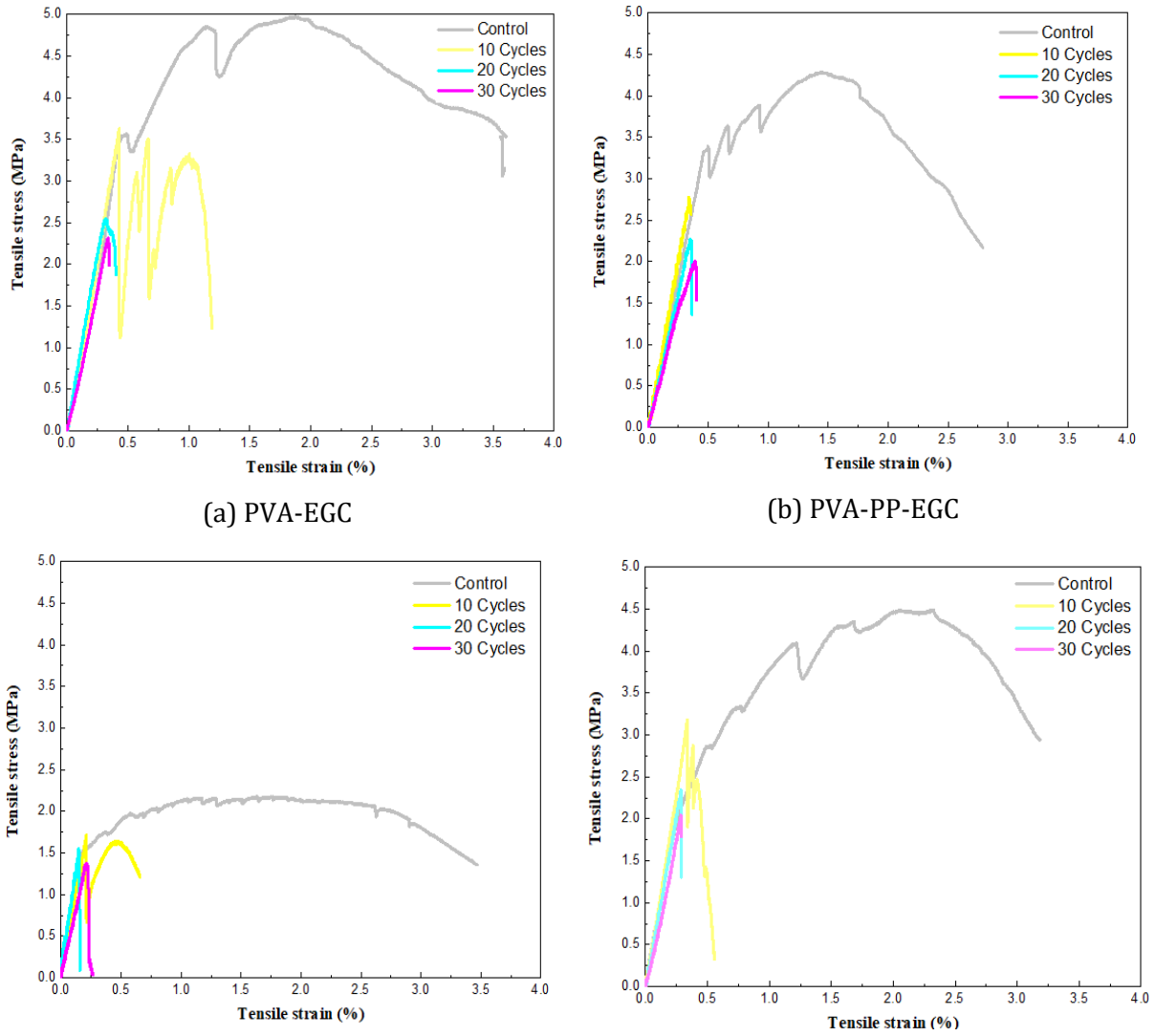

(a) PVA-EGC (b) PVA-PP-EGC

(c) PP-EGC (d) PVA-ECC

Fig. 10. The tensile stress-strain behavior of LW- ECC and EGC composite before and after undergoing thermal cycles

The effect of thermal cycling on the tensile stress and tensile ductility of green LW-ECC and LW-EGC composites is also presented in Fig. 10. The results exhibited an important decrease in tensile stress and tensile ductility of slag-based LW-EGC composites when subjected to different temperature treatments. The specimens lost their strain-hardening performance and exhibited brittle behavior similar to plain concrete under thermal cycling. Similar behavior has been observed in previous studies. The tensile strength of PVA-EGC specimens decreased by 27%, 49%, and 54% when exposed to 10, 20, and 30 cycles, respectively.

Moreover, specimens reinforced with PVA fibers exhibited a lower decrease in tensile stress and strain compared to specimens reinforced with PP fibers. This can be attributed to the deterioration of PP fibers at 200 °C, as PP fibers typically melt at around 160 °C. In contrast, polyvinyl alcohol fibers have a higher melting point above 200 °C but are considerably damaged, leading to a loss of interlayer bonding between the PVA fibers and the EGC matrix. It is worth noting that specimens reinforced with PP fibers exhibited a brittle property due to the complete melting of PP fibers at high temperatures and lost their strength. This finding aligns with the SEM observations of LW-EGC composites discussed earlier. Therefore, it was determined that the reduction in tensile strength of LW-ECC and EGC specimens under thermal cycling was more prominent than that of compressive strength, as tensile stress and strain were more susceptible to the expansion of microstructural flaws such as crack initiation and void formation during thermal curing.

3.4 Flexural Strength

The Flexural strength-deflection of green LW-ECC and EGC composites after undergoing thermal curing is presented in Fig. 11. EGC specimens reinforced by PVA fibers exhibited better flexural strength (rupture modulus) but lower deflection ability compared to specimens reinforced with PP fibers. Regardless of the fiber type, both LW-ECC and EGC specimens showed deformation-hardening behavior when tested at room temperature. The integration of PVA and PP fibers in the LW-EGC mix contributed to the control and reduction of flaws, as well as improved the interlayer connection between the fibers and cement matrix. The presence of PP and PVA fibers positively affected the deflection ability of LW-EGC composites, facilitating crack control and enhancing tension behavior in the concrete mix. The flexural performance of green LW-EGC samples, irrespective of the fiber type, significantly decreased when subjected to thermal curing at 200 °C, leading to the loss of deformation-hardening behavior. The number and width of cracks decreased with increasing thermal curing. In contrast, LW-ECC composites, with their higher porosity, allowed for steam pressure escape and exhibited fewer internal stresses, resulting in enhanced flexural strength. The flexural strength (modulus rupture) of PVA-EGC specimens decreased by 26.2%, 34.6%, and 39.3% after being subjected to 10, 20, and 30 cycle, respectively.

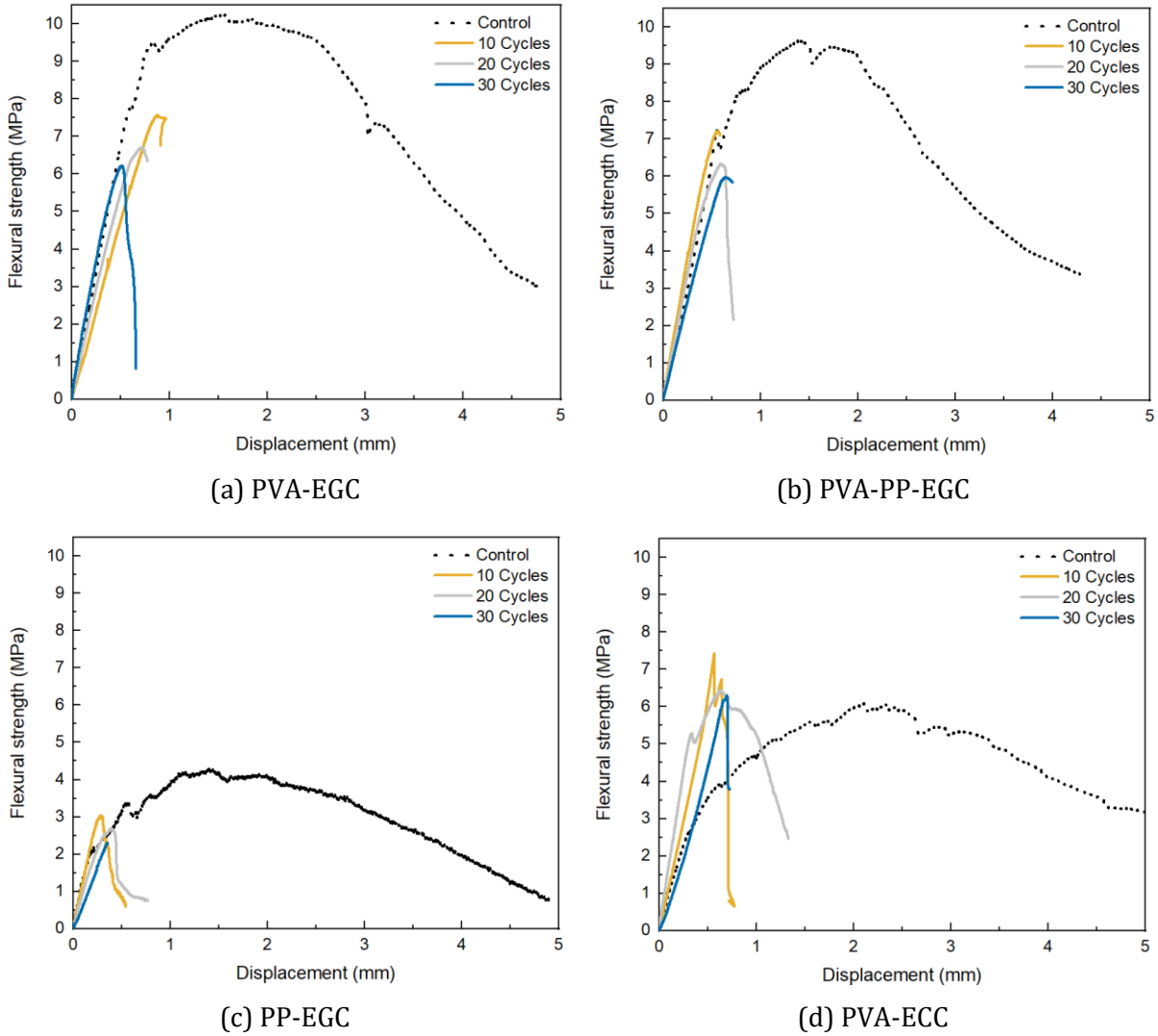

(a) PVA-EGC (b) PVA-PP-EGC

(c) PP-EGC (d) PVA-ECC

Fig. 11. Flexural strength versus deflection curves for LW- EGC and LW- ECC before and after endergoing to thermal cycles

Fig. 11 also illustrates that the residual flexural strength of PVA fiber-reinforced EGC specimens was higher than that of PP fiber-reinforced specimens after undergoing thermal curing. The degradation in flexural strength of green LW-EGC composites under thermal curing resulted in the

loss of deformation-hardening behavior, resembling plain concrete rather than traditional fiber-reinforced concrete. The degradation of fiber-matrix interfacial properties and the increase in matrix toughness contributed to the significant deterioration in flexural properties. In contrast, the flexural strength of LW-ECC specimens significantly improved with thermal curing. The flexural strength of PVA-ECC specimens increased by 21.95%, 5.8%, and 3.3% after 10, 20, and 30 thermal cycles, respectively. Nevertheless, the deflection ability of PVA-ECC specimens progressively decreased with increasing temperature variations, showing lower values compared to specimens treated at room temperature. The deterioration of PVA fibers due to temperature cycling resulted in the degradation of fiber bridging, negatively impacting the bending properties of ECC specimens.

The influence of cooling and heating treatment on the flexural, tensile, and compressive strength of green LW-ECC and EGC composites is shown in Fig. 12. The compressive and flexural strength of green LW-ECC and EGC composites remained relatively stable during thermal processing. However, the behavior of tensile strength exhibited a different trend under thermal curing conditions. This observation highlights the need for further investigation to comprehensively understand the impact of different thermal curing methods and elevated temperatures on the tensile strength of normal weight and LW-EGC composites. The experimental results obtained in this study serve as a fundamental database for understanding the properties of EGC when exposed to cooling and heating curing processes.

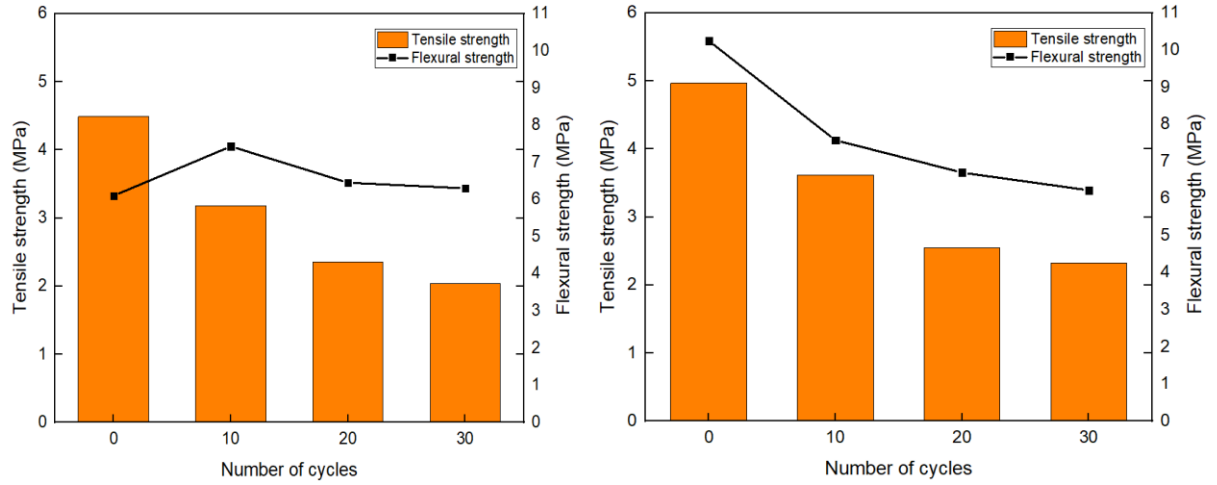

Fig. 12. Correlation between tensile strength and flexural strength at different heating-cooling cycles for LW- PVA-ECC and PVA-EGC composites

6. Conclusions and Recommendations

This research investigates the influence of two types of fibers, namely polypropylene and polyvinyl alcohol, on the mechanical behavior of slag-based EGC and ECC subjected to 0, 10, 20, and 30 heating and cooling curing cycles. LW-EGC and ECC have a density ranging from 1790 to 1870 kg/m^3, lower than that of normal-weight geopolymer concrete and normal-weight ECC. Except for the PVA-EGC composite, all the studied samples are classified as lightweight concrete. Experimental tests were conducted before and after temperature treatment, including measurements of residual mechanical performance, scanning electron microscopy, and mass loss, encompassing cyclic and static loading, deflection, failure stages, and stress-strain responses. The main contributions of this paper are as follows:

- The compressive strength of green LW-EGC specimens significantly decreased under various heating and cooling cycles due to the reduced porosity and higher density of the slag-based LW-EGC mixture. Conversely, the compressive strength of LW-ECC specimens substantially improved with increasing temperature cycling due to the enhanced reactivity of FA particles during thermal cycling.

- The addition of PP fiber in the green LW-EGC mix improved the strain properties at room temperature, providing a cost-effective alternative to the relatively expensive PVA fibers for reinforcing EGC or ECC mixtures. Irrespective of the type of composite, the tensile behavior of all the studied specimens significantly deteriorated when subjected to different thermal cycles. This behavior was attributed to the increased sensitivity of the microstructure to the expansion of internal flaws, such as starting of cracks and the development of porous problems, at various temperature curing conditions.
- The flexural properties of green LW-EGC specimens, regardless of the fiber type, were significantly reduced when subjected to various cooling and heating sequences, resulting in the complete loss of deflection-hardening properties. In contrast, the flexural strength of LW-ECC specimens remarkably enhanced under thermal cycling owing to the hydration process and accelerated pozzolanic reactions of FA. However, the deformation capacity gradually decreased due to an increase in thermal cycles, attributed to PVA fibers suffering significant damage, leading to a reduced bond between PVA fibers and the EGC matrix.
- Microstructure analysis revealed that green LW-EGC specimens experienced more severe damage than LW-ECC samples when exposed to various cooling- heating cycles. This was attributed to the higher number and porosity of ECC's microstructure, which decreased the effect of thermal treatment on the microstructure of ECC. Additionally, PVA fibers did not completely melt under thermal cycling at 200 °C, unlike PP fibers, which softened completely and disappeared during temperature curing. The microstructure of the LW-EGC specimens showed evident defects such as small cracks and a high number of capillary voids, likely due to the PP fibers leaving behind minor cracks in the EGC mixture. These defects might adversely affect the remaining mechanical behavior of LW-EGC specimens.

Future research should consider expanding the scope to other fiber types, such as steel, glass, or basalt fibers, which may offer improved high-temperature performance or other benefits. Also, extending the temperature range beyond 200°C to simulate more extreme environments like fire resistance, is crucial in many construction applications. The study could be enhanced by simulating more varied real-world conditions, such as the effects of freeze-thaw cycles or exposure to chemicals like saltwater or acids. This would give a better idea of how SEGC would perform in diverse environments. A more extended analysis of the long-term durability of SEGC is recommended, including creep, fatigue, and shrinkage characteristics under various environmental conditions. Given the sustainability angle of the research, a lifecycle assessment (LCA) could provide a more comprehensive view of the environmental impact of SEGC and ECC, comparing their carbon footprints over their entire lifespan.

References

[1] Farhan KZ, Johari MAM, Demirboğa R. Impact of fiber reinforcements on properties of geopolymer composites: A review. J Build Eng. 2021;44:102628. https://doi.org/10.1016/j.jobe.2021.102628

[2] Alcan HG, Bayrak B, Öz A, Çelebi O, Kaplan G, Aydın AC. Synergetic effect of fibers on geopolymers: Cost-effective and sustainable perspective. Constr Build Mater. 2024;414:135059. https://doi.org/10.1016/j.conbuildmat.2024.135059

[3] Abdalla JA, Hawileh RA, Bahurudeen A, Jyothsna G, Sofi A, Shanmugam V, et al. A comprehensive review on the use of natural fibers in cement/geopolymer concrete: A step towards sustainability. Case Stud Constr Mater. 2023;22:e02244. https://doi.org/10.1016/j.cscm.2023.e02244

[4] Wasim M, Ngo TD, Law D. A state-of-the-art review on the durability of geopolymer concrete for sustainable structures and infrastructure. Constr Build Mater. 2021;291:123381. https://doi.org/10.1016/j.conbuildmat.2021.123381

[5] Duan P, Yan C, Zhou W, Ren D. Fresh properties, compressive strength and microstructure of fly ash geopolymer paste blended with iron ore tailing under thermal cycle. Constr Build Mater. 2016;118:76-88. https://doi.org/10.1016/j.conbuildmat.2016.05.059

[6] Duan P, Yan C, Zhou W. Compressive strength and microstructure of fly ash-based geopolymer blended with silica fume under thermal cycle. Cem Concr Compos. 2017;78:108-19. https://doi.org/10.1016/j.cemconcomp.2017.01.009

[7] Humur G, Çevik A. Effects of hybrid fibers and nanosilica on mechanical and durability properties of lightweight engineered geopolymer composites subjected to cyclic loading and heating-cooling cycles. Constr Build Mater. 2022;326:126846. https://doi.org/10.1016/j.conbuildmat.2022.126846

[8] Lin Z, Xu W, Wang W, Zhang J, Wang H, Wang R. Experimental study on hydraulic and macro-mechanical property of a mortar under heating and cooling treatment. J Adv Concr Technol. 2016;14:261-70. https://doi.org/10.3151/jact.14.261
[9] An M, Huang H, Wang Y, Zhao G. Effect of thermal cycling on the properties of high-performance concrete: Microstructure and mechanism. Constr Build Mater. 2020;243:118310. https://doi.org/10.1016/j.conbuildmat.2020.118310
[10] Das D, Gołąbiewska A, Rout PK. Geopolymer bricks: The next generation of construction materials for sustainable environment. Constr Build Mater. 2024;445:137876. https://doi.org/10.1016/j.conbuildmat.2024.137876
[11] Chelluri S, Hossiney N. Performance evaluation of ternary blended geopolymer binders comprising of slag, fly ash and brick kiln rice husk ash. Case Stud Constr Mater. 2024;20:e02918. https://doi.org/10.1016/j.cscm.2024.e02918
[12] Debnath K, Das D, Rout PK. Effect of mechanical milling of fly ash powder on compressive strength of geopolymer. Mater Today Proc. 2022;68:242-9. https://doi.org/10.1016/j.matpr.2022.08.321
[13] Alanazi H, Hu J, Kim YR. Effect of slag, silica fume, and metakaolin on properties and performance of alkali-activated fly ash cured at ambient temperature. Constr Build Mater. 2019;197:747-56. https://doi.org/10.1016/j.conbuildmat.2018.11.172
[14] Sbahieh S, McKay G, Al-Ghamdi SG. Comprehensive analysis of geopolymer materials: Properties, environmental impacts, and applications. Materials. 2023;16:7363. https://doi.org/10.3390/ma16237363
[15] Wang F, Ma J, Ding Y, Yu J, Yu K. Engineered geopolymer composite (EGC) with ultra-low fiber content of 0.2%. Constr Build Mater. 2024;411:134626. https://doi.org/10.1016/j.conbuildmat.2023.134626
[16] Subramaniam DN, Sathiparan N. Comparative study of fly ash and rice husk ash as cement replacement in pervious concrete: Mechanical characteristics and sustainability analysis. Int J Pavement Eng. 2023;24:2075867. https://doi.org/10.1080/10298436.2022.2075867
[17] Elmessalami N, El Refai A, Abed F. Fiber-reinforced polymers bars for compression reinforcement: A promising alternative to steel bars. Constr Build Mater. 2019;209:725-37. https://doi.org/10.1016/j.conbuildmat.2019.03.105
[18] Ling Y, Wang K, Li W, Shi G, Lu P. Effect of slag on the mechanical properties and bond strength of fly ash-based engineered geopolymer composites. Compos Part B Eng. 2019;164:747-57. https://doi.org/10.1016/j.compositesb.2019.01.092
[19] Humur G, Çevik A. Mechanical characterization of lightweight engineered geopolymer composites exposed to elevated temperatures. Ceram Int. 2022;48:13634-50. https://doi.org/10.1016/j.ceramint.2022.01.243
[20] ASTM. ASTM C109/C109M-02: Standard test method for compressive strength of hydraulic cement mortar. West Conshohocken, PA, USA: ASTM International; 2002.
[21] Bhat PS, Chang V, Li M. Effect of elevated temperature on strain-hardening engineered cementitious composites. Constr Build Mater. 2014;69:370-80. https://doi.org/10.1016/j.conbuildmat.2014.07.052
[22] Rokugo K. Recommendations for design and construction of high performance fiber reinforced cement composites with multiple fine cracks (HPFRCC). Tokyo, Japan: Japan Society of Civil Engineers, Concrete Committee; 2008.
[23] Şahmaran M, Lachemi M, Hossain KM, Li VC. Internal curing of engineered cementitious composites for prevention of early age autogenous shrinkage cracking. Cem Concr Res. 2009;39:893-901. https://doi.org/10.1016/j.cemconres.2009.07.006
[24] Li Y, Li W, Deng D, Wang K, Duan WH. Reinforcement effects of polyvinyl alcohol and polypropylene fibers on flexural behaviors of sulfoaluminate cement matrices. Cem Concr Compos. 2018;88:139-49. https://doi.org/10.1016/j.cemconcomp.2018.02.004
[25] Lin J-X, Song Y, Xie Z-H, Guo Y-C, Yuan B, Zeng J-J, et al. Static and dynamic mechanical behavior of engineered cementitious composites with PP and PVA fibers. J Build Eng. 2020;29:101097. https://doi.org/10.1016/j.jobe.2019.101097
[26] Aygörmez Y, Canpolat O, Al-Mashhadani MM, Uysal M. Elevated temperature, freezing-thawing and wetting-drying effects on polypropylene fiber reinforced metakaolin-based geopolymer composites. Constr Build Mater. 2020;235:117502. https://doi.org/10.1016/j.conbuildmat.2019.117502
[27] Şahmaran M, Lachemi M, Li VC. Assessing mechanical properties and microstructure of fire-damaged engineered cementitious composites. ACI Mater J. 2010;107. https://doi.org/10.14359/51663759
[28] Zhou X, Li Z. A constitutive model for fiber-reinforced extrudable fresh cementitious paste. Comput Concr. 2011;8:371-88. https://doi.org/10.12989/cac.2011.8.4.371
[29] ACI Committee. Guide for selecting proportions for high-strength concrete using Portland cement and other cementitious materials. Farmington Hills, MI: ACI Committee; 2008.
[30] Nath S, Kumar S. Influence of iron-making slags on strength and microstructure of fly ash geopolymer. Constr Build Mater. 2013;38:924-30. https://doi.org/10.1016/j.conbuildmat.2012.09.070

[31] Nath S, Kumar S. Influence of granulated silico-manganese slag on compressive strength and microstructure of ambient cured alkali-activated fly ash binder. Waste Biomass Valorization. 2019;10:2045-55. https://doi.org/10.1007/s12649-018-0213-1

[32] Fang G, Ho WK, Tu W, Zhang M. Workability and mechanical properties of alkali-activated fly ash-slag concrete cured at ambient temperature. Constr Build Mater. 2018;172:476-87. https://doi.org/10.1016/j.conbuildmat.2018.04.008

[33] Mohammedameen A, Gülşan ME, Alzeebaree R, Çevik A, Niş A. Mechanical and durability performance of FRP-confined and unconfined strain-hardening cementitious composites exposed to sulfate attack. Constr Build Mater. 2019;207:158-73. https://doi.org/10.1016/j.conbuildmat.2019.02.108

[34] Gülşan ME, Mohammedameen A, Şahmaran M, Niş A, Alzeebaree R, Çevik A. Effects of sulphuric acid on mechanical and durability properties of ECC confined by FRP fabrics. Adv Concr Constr. 2018;6:199.

[35] Irshidat MR, Al-Nuaimi N, Rabie M. Hybrid effect of carbon nanotubes and polypropylene microfibers on fire resistance, thermal characteristics and microstructure of cementitious composites. Constr Build Mater. 2021;266:121154. https://doi.org/10.1016/j.conbuildmat.2020.121154